International Journal of Mining and Geo-Engineering

IJMGE

IJMGE 54-2 (2020) 179-183

DOI: 10.22059/ijmge.2019.278501.594793

Numerical Investigation of the Impact of Geomechanical Parameters of Formations on Well Integrity of One of the Iranian Oil Fields

Eissa Khodami [a], Ahmad Ramezanzadeh [a], Mehdi Noroozi [a,*], Mohammad Mehrad [a]

[a] *Faculty of Mining, Petroleum and Geophysics Engineering, Shahrood University of Technology, Shahrood, Iran*

Article History:

Received: 29 March 2019,
Revised: 23 August 2019,
Accepted: 29 August 2019.

ABSTRACT

Well integrity is defined as the application of technical and operational solutions to reduce the uncontrollable risk of fluids leakage in the well lifetime. In any drilling and production operation, lack of knowledge about geomechanical behavior of the surrounding formations is considered as a major risk. Therefore, in-situ stress conditions and mechanical properties of formations are important factors in well integrity studies. In this paper, a 3D finite element model was built to simulate the integrity of wells. An FEM analysis was used to investigate the plastic deformation in cement and the Von Mises failure criterion inside the casings under different stress conditions, and to study the mechanical properties of the formation. A clear increase in plastic strain in the cement and Von Mises stress inside the casings was observed with increasing the ratio of horizontal to vertical stress in orthotropic and isotropic conditions as well as with increasing the difference between horizontal stresses in anisotropic conditions. When conducting the translation error sensitivity analysis, the impact of major mechanical parameters of the formation was evaluated as well. The results showed that by increasing Young's modulus, cement became hard and brittle. Meanwhile, an increase in the Poisson ratio led to plastic behavior. The maximum plastic strain was found at the cement-casing boundary due to the presence of a lower cement-formation friction value. The highest Von Mises stress value in the casings was also produced parallel toward the minimum horizontal stress. Additionally, with an increase in the cohesion and friction angle of formation, the cement became harder, and consequently, the safety factor for the casings increased.

Keywords : *Well integrity, Geomechanical parameters, Numerical method, Plastic strain*

1. Introduction

Base on NORSOK D-010, well integrity is defined as the application of technical, operational, and organizational solutions in order to decrease the risk of uncontrolled diffusion of formation fluids over the lifespan of wells. Controlling the well integrity in all related operations is the most important concern for operators all over the world. The high costs of old wells' maintenance and the higher costs of new wells make well integrity to be an important factor in the life of the well [1]. It is known that factors such as wellbore instability, corrosion, cement bond decline, changing pressure envelopes, expansion, and contraction result in the loss of well integrity. Thus, estimating the integrity of existing wellbores is necessary for optimizing productivity and adding price [2]. Therefore, well barriers are applied to prevent fluid leakage and reduce the risks related to drilling, production, and interposition activities. Well barriers are defined as covers of one or several dependent barrier elements and can prevent unintentional flow-out of fluids or gases from the well into the formation or surface [1]. In order to apply the formation as part of the barrier cover, it should be impermeable and without any open fractures/faults, and should not allow gasses or fluids permeation through time [3]. Knowing the state of subsurface in-situ stresses and stress changes throughout the life of the well is essential for investigating the stability of the well and well integrity [4]. The balance between concentrated stress on the wellbore and rock strength is of the initial condition for the stability of wells in the drilling phase. Well instability occurs when effective stresses overcome rock strength [5]. Due to mechanical actions, drilling a well induces stresses in the region of the wellbore, whose rate depends on the position and distance from the well. Also, during the exploitation, the pressure of the reservoir is drained, and the rocks near the well are compressed, which will result in a change in the regime of stress and the creation of induced stresses. Induced stresses around the well that are causing instability and failure in the formation, and subsequently in the wall of the well, should be reduced by cementing and implanting casings inside the wells. Accordingly, the cementing and casing operations are to be considered as the two most important steps in the well design. Thus, in order to make cost-effective decisions in these two steps, the effects of geomechanical properties of the formation such as Young’s modulus, cohesion, friction angle, Poisson’s ratio, and in-situ stresses on cementing and casing of the wells (or in other words, the well integrity) should be evaluated.

Finite element models are used to study the behavior of well integrity under reservoir conditions in different fields. The tube buckling analysis was conducted to evaluate the long-term integrity of a hydrocarbon well by using the ABAQUS software in 2011 by Topini et al. [6]. Li et al. (2012) examined the mechanical fracture analysis of cement under an in-situ stress field. They found that when the in-situ stress is relatively large, the increase in internal pressure can provide an appropriate function in the stability of the coating [7]. Himmelberg (2014) performed a numerical study on well integrity during the drilling and well completion stages. In this study, the mechanical influences of the cement sheath-casing-formation were studied. In addition, the effect of increased Young’s modulus of cement during cement hardening and degrading stages was simulated [4]. Feng et al. (2016) presented a 3D

* Corresponding author. *E-mail address:* mnoroozi.mine@gmail.com (M. Noroozi).

model of the loss of the cement-casing bond. In their modeling, they designed a model to simulate crack growth in cement. The results indicated that the width and peripheral growth depend on the in-situ stress configuration, initial cracks around the casing, and the characteristics of the cement and the formation [8].

In the present paper, we focused on a well drilled into one of Iran's Southwestern Oil Fields, and used a three-dimensional numerical Finite Element Model via the ABAQUS Software, to investigate well integrity. Among the parameters that affect the integrity of the well, this paper has focused on the formation properties. In the following, the formation geomechanical parameters were used to analyze the stability of the well of interest during the drilling and well completion stages. Finally, the sensitivity analyses and parametric studies were performed to investigate the impact of in-situ stresses and mechanical properties of the formation on well integrity. Various in-situ stress configurations, including isotropic, orthotropic, and anisotropic, were taken into account. Under isotropic and orthotropic conditions, an increase in the horizontal to vertical stress ratio was contributed to the higher plastic strain in the well. However, under an anisotropic condition, increasing the difference between the horizontal stress components would increase the plastic strain of the well. Also, well integrity increases with increasing Young's modulus, friction angle, and the cohesion of the formation.

2. Geomechanical factors affecting well integrity

The geomechanics studies have been conducted through geomechanical analyses to unveil the geological responses of the formation to the conditions created by oil wells. Nowadays, in many drilling, completion, and production operations, the lack of awareness about the geomechanical conditions of the environment is a major risk. Expanding a stable geomechanical analysis of well integrity reduces the existing risk to an acceptable level, and provides other valuable benefits during the optimal lifetime of the well. Any well excavated can be considered as a rocky mechanical test. Through the subsurface media, there are various stress components exerting the pressure on the rocks below the surface of the earth. By drilling a well, the present state of stress is disrupted, which is a function of the location and distance from the well's wall. The response of the formation in the well to this turbulence is a function of rock resistance and the stress strength. The geomechanical parameters used in this research include elastic properties of the formation, such as Young's modulus and Poisson's coefficient, as well as available in-suit stresses such as vertical or overload stresses and horizontal stresses in minimum and maximum states, and plastic parameters of the formation, including cohesion and internal friction angle.

3. Numerical modeling of well integrity

The behavior of the cement sheath in the reservoir range can be studied through finite element modeling [9]. In this research, a finite Element Method (FEM) was used to numerically evaluate the wellbore stability and the integrity of the cement sheath. In this method, the simulation was performed by dividing the environment into a system of blocks. The finite element method allows comparing complicated modeling with laboratory conditions, and its results are very accurate [10, 11]. The properties of the materials used in the modeling are presented in Table 1. These values were taken into account based on the behavioral model. These values are derived from available logs and the use of existing empirical relationships. The in-situ stress state was defined to be orthotropic for the studied depth (3800 m) with vertical stress of 95 MPa and minimum and maximum horizontal stresses of 62 and 95 MPa, respectively. The vertical stress was calculated using the density log, and the horizontal stress components were measured using a methodology based on the poroelastic theory. According to the research objectives, a hydro-mechanical couple was intended to investigate the effect of pore pressure on the amounts of the principal stresses.

Table 1. Properties of materials used in the modeling [12].

Material	Density (Kg/m^3)	Young's modulus (GPa)	Poisson's ratio	Cohesion (MPa)	Friction angle
Formation	2560	27	0.29	25	42
Cement	1893	6.38	0.2	7.14	26
Casing	7850	210	0.3	-	-

The overall dimensions of the constructed model were 10m*10m*5m, and a well with a diameter of 21.2852 cm was drilled at the center of the model. The thickness of the cement and the casing were 4.2926cm and 0.919cm, respectively. The meshing was in accordance with Fig. 1, meaning that the closer we got to the well, the smaller the elements would get. This model consisted of 45800 elements and 53691 nodes, of which 37000 elements were of the C3D8RP type, 8000 elements of the C3D8R type, and 800 elements were of the C3D6P type. In this study, the optimum model and the mesh sizes were obtained through trial and error to estimate the in-situ stresses in the balanced state.

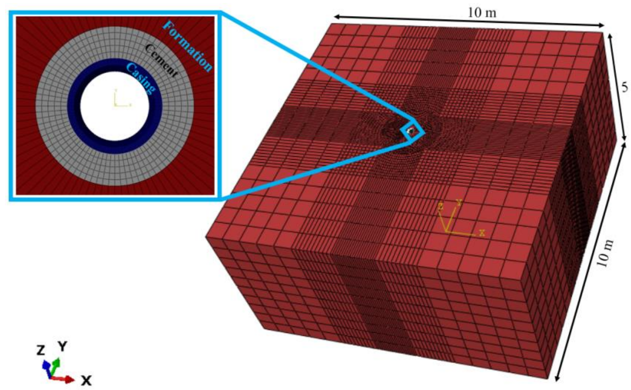

Fig. 1. Mesh dimensions of the near wellbore region of the mapped mesh.

The model was made in three stages of geostatic, drilling, and completion. In the geostatic stage, the formation was balanced under the initial boundary conditions, such as in-situ stresses and pore pressure. Fig. 2 shows the effective stress counters in the Z direction at the geostatic stage. According to the gravitational acceleration of earth, as the depth increased, the stresses increased in the vertical direction.

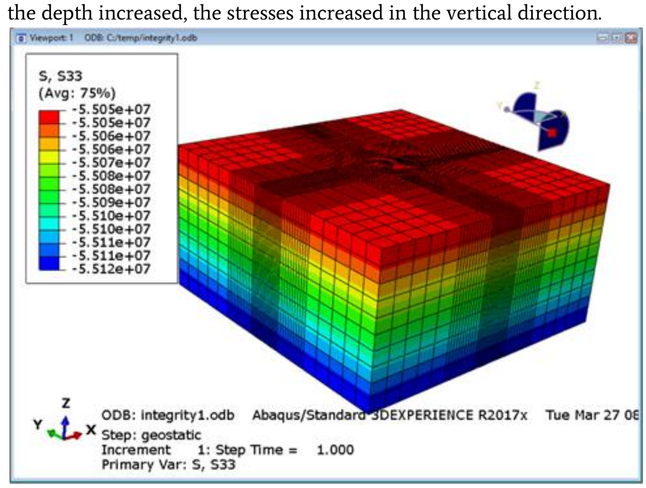

Fig. 2. Effective stress counters in the geostatic stage.

In the drilling stage, a part of the formation (21.28 cm in diameter), was removed from the analysis, which, as the drilling takes place, the hydrostatic pressure of the mud at the amount of 42 MPa was applied to the inner wall of the well. In the stage of completion, the cement and casing were added to the model, and the interface between cement-formation and cement-casing was activated. The properties of these interfaces are shown in Table 2. In order to construct the contact surfaces in the ABAQUS Software, two types of contact between the common surfaces were considered: friction and vertical. For the sake of the frictional and vertical contact surfaces, Coulomb's friction law and the penalty-based hard contact (with properties given in Table 2) were used, respectively. In this paper, according to the research studies reported by Capasso and Musso (2010), the shear stress developed between the cement-casing was assumed to be 0.1 of the shear stress between the formation-cement.

Table 2. Properties of the interface [13, 6].

Contact surfaces	Shear stress (KPa)	Friction coefficient	Vertical contact
Cement-formation	200	0.5	Hard
Cement-casing	20	0.3	Hard

The Von Mises failure criterion indicates that if the combination of the three main stresses exceeds the material yield strength, the failure will occur. This criterion is in accordance with equation (1). In this equation, σ_1 is the maximum main stress, σ_2 is the mean main stress, and σ_3 is the minimum main stress [14].

$$\sigma_{VM} = \sqrt{\frac{(\sigma_1-\sigma_2)^2+(\sigma_2-\sigma_3)^2+(\sigma_3-\sigma_1)^2}{2}} \quad (1)$$

Equation 2 represents the casing-safety factor (SF_{casing}), in which S_y is the steel yield strength used in the fabrication of casing (552 MPa), and σ_{VM} is the maximum Von Mises stress created in the casing.

$$SF_{casing} = \frac{\sigma_{VM}}{S_y} \quad (2)$$

The main objective of this FEA was to show the plastic deformation phenomenon of the cement-formation set after the completion of the well. Plasticity of rocks and cement were measured in this FEA model as the equivalent plastic strain, PEEQ — the maximum total plastic strain. Mathematically, the plastic strain is in accordance with equation (3). In this equation, ε_{ij}^p is the plastic strain rate tensor, and t is time [14].

$$PEEQ = \int_0^t \sqrt{\frac{2}{3}\sum_{ij=1,2,3}(\varepsilon_{ij}^p \varepsilon_{ij}^p)}\,dt \quad (3)$$

The base model was placed under the conditions of orthotropic stress. The chosen stress values are presented in Table 3 in red. Fig. 3 (a) shows the variations of the Von Mises stress in the casing, and Fig. 3 (b) shows the plastic strain in the cement after the completion of the well. The horizontal minimum and maximum stresses were applied to the model in directions X and Y, respectively. It can be observed from Fig. 3 that the plastic strain was mainly concentrated in the direction of maximum horizontal stress and the maximum stress of the Von Mises in the direction of minimum horizontal stress. The contact surface between the cement and the casing had less friction than the cement and the formation; therefore, the concentration of the plastic strain was higher on that surface.

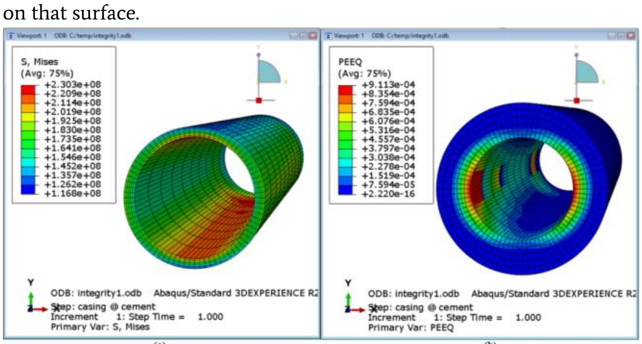

Fig. 3. The variations of the Von Mises stress in the casing (a) and plastic strain in the cement (b).

4. The effect of in-situ stresses on well integrity

As we know, the formation system, cement, and casing tolerate the stresses that originate from the in-situ stress. These pressures include vertical, maximum horizontal, and minimum horizontal stresses. Many researchers consider equal horizontal stresses values to simplify the problem, but in fact, these two stresses are not always equal. This means that the assumption that the in-situ stresses are isotropic cannot be used to analyze the stress field of this system. Elastic analytical models have been used under anisotropic conditions of in-situ stresses [15, 16]. Elastic-plastic analytical models have also been presented under isotropic conditions of in-situ stresses [17, 18]. As observed in Table 3, the distribution of in-situ stresses is analyzed in terms of the susceptible in the orthotropic and isotropic form. In table 3, σ_v, σ_H, and σ_h are vertical, maximum, and minimum horizontal stresses, respectively. Orthotropic materials have two or three axes of symmetry perpendicular to each other, and in general, the mechanical properties of the material throughout each of these axes are different from the other axis. According to Table 2, four states have been considered for orthotropic conditions. State 2 shows the isotropic conditions. When the formation is in the isotropic condition, its properties, including stress, are independent of the direction and are equal in the three directions of X, Y, and Z.

Table 1. In-situ stresses of the formation in orthotropic and isotropic conditions.

Case	Stress Conditions	$\sigma_v\,(Mpa)$	$\sigma_H-\sigma_h\,(Mpa)$	σ_H/σ_V	σ_h/σ_V
1	Orthotropic $\sigma_H=\sigma_h \prec \sigma_v$	95	0	0.65	0.65
		95	0	0.75	0.75
		95	0	0.85	0.85
2	Isotropic $\sigma_H=\sigma_h=\sigma_v$	95	0	1	1
3	Orthotropic $\sigma_H=\sigma_h \succ \sigma_v$	95	0	1.1	1.1
		95	0	1.2	1.2
		95	0	1.3	1.3
4	Orthotropic $\sigma_H=\sigma_v \succ \sigma_h$	95	14	1	0.85
		95	24	1	0.75
		95	33	1	0.65
5	Orthotropic $\sigma_H \succ \sigma_v=\sigma_h$	95	14	1.15	1
		95	24	1.25	1
		95	33	1.35	1

The values of Von Mises stress increased with increasing the stress ratio, considering the horizontal stresses as the main factors influencing on wellbore stability. Plastic strain in the cement is increased by increasing stresses around wellbore. The induction of the cement sheath decreased the safety factor (Fig. 4 (a)). In addition, the Von Mises stress in the casing increased according to Fig. 4 (b).

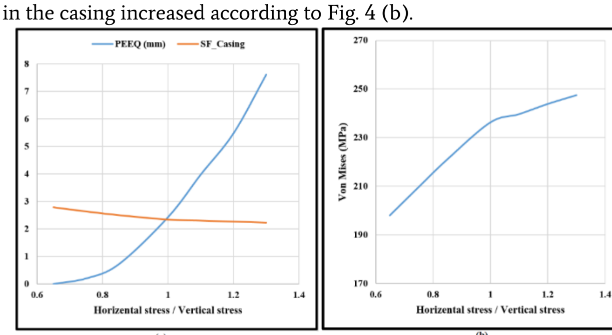

Fig. 4. The safety factor of the casing and plastic strain in the cement. (a) The Von Mises stress in the casing; (b) relative to the ratio of horizontal to vertical stresses.

According to Fig. 5, as the difference between horizontal stresses increases, the Von Mises stress enhances in the casing (a), and the maximum plastic strain increases in the cement (b).

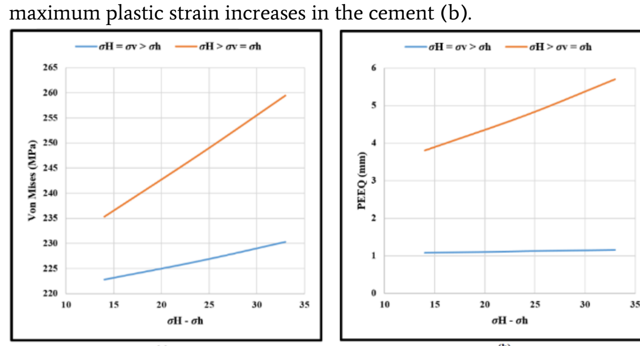

Fig. 5. The Von Mises stress in the casing (a) and plastic strain in the cement (b) relative to the difference between horizontal stresses.

According to Table 4, in anisotropic conditions, the properties of the formation, including stress, vary in different directions; thus, the states 1 to 3 are considered for the analysis of these conditions. Horizontal stress differences are sensitized in three states of 14, 24, and 33 MPa. In other words, the horizontal stress changes at least to the stage where σ_H and σ_h are equal and converge from an anisotropic condition to an orthotropic one.

Table 4. In-situ stresses of the formation in the anisotropic conditions.

case	Stress Condition	σ_v (MPa)	$\sigma_H - \sigma_h$ (MPa)	σ_H/σ_V	σ_h/σ_V
1	Anisotropic ($\sigma_h \prec \sigma_H \prec \sigma_v$)	95	14	0.85	0.7
		95	24	0.9	0.65
		95	33	0.95	0.6
2	Anisotropic ($\sigma_H \succ \sigma_h \succ \sigma_v$)	95	14	1.3	1.15
		95	24	1.35	1.1
		95	33	1.4	1.05
3	Anisotropic ($\sigma_H \succ \sigma_v \succ \sigma_h$)	95	14	1.05	0.9
		95	24	1.1	0.85
		95	33	1.15	0.8

According to Fig. 6, the plastic strain in the cement and the Von Mises stresses in the casings increase by increasing the difference between horizontal stresses, and consequently, the casing safety factor decreases according to the Von Mises criterion. After conducting the sensitivity analysis on the main stresses distribution conditions in the formation, it can be concluded that the most critical condition for casing safety factor is related to the complete anisotropy conditions, in which $\sigma_H > \sigma_h > \sigma_v$, and when the horizontal stresses are greater than the vertical stresses, the safety factor of the casing is minimum. The maximum strain in the boundary elements between the cement and the casing is created, which causes the separation and creation of a channel for passing the fluid flow. Therefore, in the design of cement slurry, special additives should be considered to bind the slurry to the casing and to increase the surface friction.

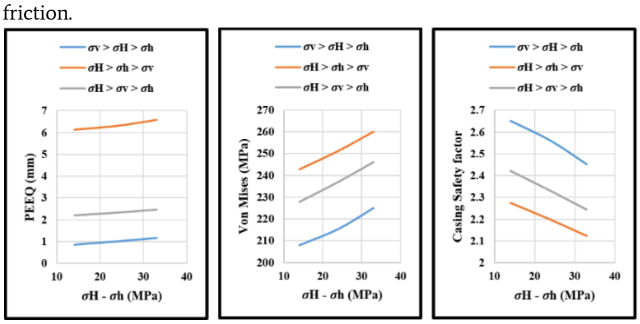

Fig. 6. Plastic strain in the cement, the Von Mises stress in the casing, and Safety factor of the casing relative to the difference between horizontal stresses in anisotropic conditions.

5. The effect of mechanical parameters of the formation

The simplest structural model for describing rock behavior is the linear elastic model, which is the basis of calculations for rock mechanics. This theory is based on Hooke's law, which depends on the concepts of stress and strain. Young's modulus and Poisson's coefficient are two parameters needed to describe the elastic response of any material, including the rock. Modeling the plastic behavioral criterion relative to elasticity and considering the two parameters of cohesion and friction angle will provide more satisfactory and acceptable results. First, by constructing a single-dimensional geomechanical model of the reservoir, the parameters of the Mohr-Coulomb Behavioral Model are calculated, and then, according to Table 5, the elastoplastic parameters of the formation are sensitized to examine well integrity.

Table 5. Selected values for the sensitivity analysis.

Case	a	b	c	d
E (GPa)	20 47 60	47	47	47
υ	0.29	0.15 0.29 0.45	0.29	0.29
C (MPa)	25	25	20 25 30	25
φ (degree)	42	42	42	30 42 50

One of the important factors in the design of the pipe is the access to the properties of the formation. Therefore, predicting the safety of the casing in various formations is of great importance.

Fig. 7 shows the changes in the plastic strain created at the well completion stage from the top view. Fig. 7 (a), in the case of rock mass cohesion, is 30 MPa, and the cohesion of Fig. 7 (b) reduced to 20 MPa. It is also clear from the figure that, in addition to increasing the plastic strain in the cement, the elements of the formation around the well will reach the plastic stage by reducing the cohesion of the rock.

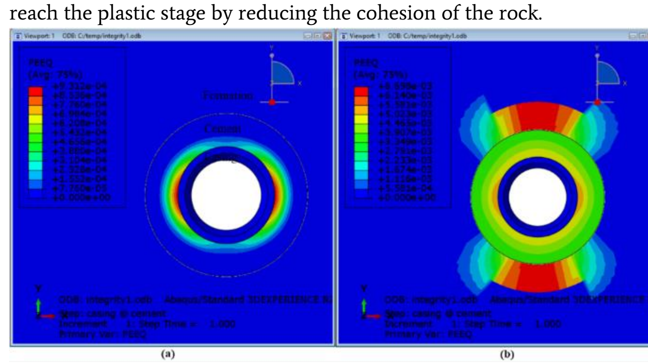

Fig. 7. The plastic strain created at the well completion stage (rock mass cohesion 30 MPa (a) and 20 MPa (b)).

Fig. 8 shows the bar diagram of the changes in the cement plastic strain and the casing safety factor compared to the changes in mechanical parameters of the formation in different states. The cement becomes harder, and the casing becomes safer by increasing Young's modulus, cohesion and friction angle, and the reduction of Poisson's coefficient. In addition to these, Young's modulus of the formation, among other mechanical parameters, has a greater effect on the safety of the cement and casing. By increasing the formation's Young's modulus, the plastic strain in cement and formation decreases. Therefore, it can be concluded that in soft rocks, the plastic strain around the well is higher than that of the hard rocks. As shown in the figure, the changes in the formation of plastic strain versus Young's modulus show a linear trend. The internal friction angle is the second most important parameter of the formation. This parameter indicates the ability of the formation for confronting to shear stresses. By increasing the friction angle of the formation, the plastic strain decreases with a further decline in the formation cohesion. The process of changing this parameter follows polar relations with a high confidence level.

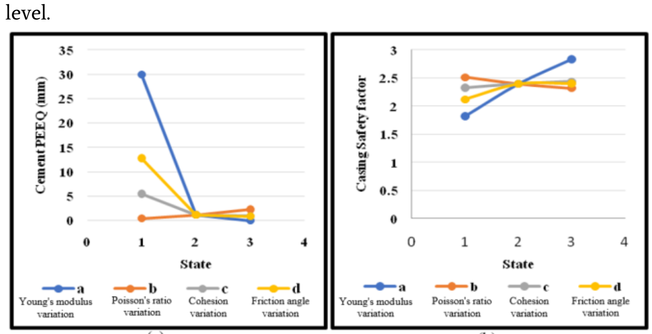

Fig. 8. The bar diagram of (a) variations in the cement plastic strain and (b) the casing safety factor, in comparison to variations of the mechanical parameters of the formation.

6. Conclusion

Finite element analysis (FEA) and sensitivity analysis (SA) were employed on the geomechanical parameters, and their effects on well integrity were assessed. The following conclusions can be drawn from this work:

1. Plastic strain in the cement and Von Mises stress created in the

casing is increased, and as a result, the safety factor of the casing is decreased by increasing the ratio of the horizontal to vertical stress in orthotropic and isotropic conditions.

2. In anisotropic conditions, the plastic strain in the cement and Von Mises stress in the casing increased by increasing the difference between horizontal stresses and decreased the safety factor of the casing.
3. Through examining the safety of the casing under different conditions, the most critical event occurred in conditions where ($\sigma_H > \sigma_h > \sigma_V$), in which the safety factor reached its minimum value (2.123). The worst state, in terms of the formation of the strain of plastic, was the condition where ($\sigma_H = \sigma_h > \sigma_V$). In this case, the plastic strain created in the cement raised to 7.617 mm.
4. The maximum plastic strain at the boundary between the cement and casing was created due to less friction than cement-formation, and the maximum Von Mises stress created in the conditions of anisotropy occurred toward the minimum horizontal stress.
5. The cement became harder and more fragile, and the safety factor for the casing increased with the increase of Young's modulus, cohesion, and the friction angle of the formation. In addition, the cement showed a plastic behavior, and the safety factor of casing decreases by increasing Poisson's coefficient.

The safety factor was more than one in all in-situ stress conditions and mechanical parameters of the formation, indicating that the well in the casing section was safe, and its integrity was not threatened.

REFERENCES

[1] N. Standard. (2004). Well integrity in drilling and well operations, D-010, rev, vol. 3.

[2] D. U. Etetim. (2013). Well Integrity behind casing during well operation. Alternative sealing materials to cement, Institutt for petroleumsteknologi og anvendt geofysikk.

[3] Sangesland, S., Rausand, M., Torbergsen, H., Haga, H., Aadnøy, B., Sæby, J., Johnsen, S., Lundeteigen, M. (2012). An Introduction to well integrity, Rev 0.

[4] N. C. Himmelberg. (2014). Numerical simulations for wellbore stability and integrity for drilling and completions. Missouri University of Science and Technology.

[5] M. Shahri, J. J. Schubert, and M. Amani. (2005) Detecting and modeling cement failure in high-pressure/high-temperature (HP/HT) wells, using finite element method (FEM), in International Petroleum Technology Conference.

[6] C. Topini, F. Bertolo, G. Capasso, and S. Mantica. (2011). Buckling analysis for the long-term integrity evaluation of a hydrocarbon well, in Proc. Simulia Customer Conference, Barcelona, Spain.

[7] Li, Y., Yuan, J., Qi, F., Liu, S., Wang, Z., & Qu, C. (2012, January). Analysis of cemented casing mechanical failure under arbitrary in-situ stress field coupling effects of downhole pressure and temperature. In IADC/SPE Asia Pacific Drilling Technology Conference and Exhibition. Society of Petroleum Engineers.

[8] Feng, Y., Podnos, E., & Gray, K. E. (2016, June). Well integrity analysis: 3D numerical modeling of cement interface debonding. In 50th US Rock Mechanics/Geomechanics Symposium. American Rock Mechanics Association.

[9] Z. Shen and F. E. Beck. (2012). Three-dimensional modeling of casing and cement sheath behavior in layered, nonhomogeneous formations, in IADC/SPE Asia Pacific Drilling Technology Conference and Exhibition.

[10] M. G. Haider, J. Sanjayan, and P. G. Ranjith. (2012). Modeling of a well-bore composite cylinder system for cement sheath stress analysis in geological sequestration of CO2, in 46th US Rock Mechanics/Geomechanics Symposium.

[11] S. Abaqus. (2017). Abaqus Version 2017 Analysis User's Guide.

[12] National Iranian South Oil Company, geological report, 2009.

[13] G. Capasso and G. Musso. (2010). Evaluation of Stress and Strain Induced by the Rock Compaction on a Hydrocarbon Well Completion Using Contact Interfaces with Abaqus," in Proc. ABAQUS Users' Conference, Providence RI, USA.

[14] H. Arias. (2013). Use of finite-element analysis to improve well cementing in HTHP conditions. Texas A&M University.

[15] J. Fan and B. Yue. (1997). Analysis of surface loading on casing and cement sheath under nonuniform geologic stress, JOURNAL-UNIVERSITY Pet. CHINA Nat. Sci. Ed., vol. 21, pp. 46–48.

[16] F. Jun, Z. Huaiwen, Y. Boqian, and S. Yufeng. (1995). Analysis of Loading Propekty of Casing and Cement Sheath Under Nonuniform Geologic Stress [J], J. Univ. Pet. China, vol. 6.

[17] L. Jun, C. Mian, L. Gonghui, and Z. Hui. (2005). Elastic-plastic analysis of casing-concrete sheath-rock combination, Acta Pet. Sin., vol. 26, no. 6, pp. 99–103.

[18] J. Li, M. Chen, H. Zhang, and S.-L. Zi. (2005). Effects of cement sheath elastic modulus on casing external collapse load, Shiyou Daxue Xueban Ziran Kexue Ban(Journal Univ. Pet. China Nat. Sci. Ed., vol. 29, no. 6, pp. 41–44.